A TRANSITION FLOW REGIME ON STEPPED SPILLWAYS THE FACTS

H. Chanson

Department of Civil Engineering, The University of Queensland,

Brisbane QLD 4072, Australia

Fax: (61 7) 33 65 45 99 - E-mail: h.chanson@mailbox.uq.edu.au

Abstract: The stepped channel design have been used since more than 3,000 years. It is understood that low flows behave as successions of free-jets (i.e. nappe flow) while large discharges skim over the pseudo-bottom formed by the step edges. For a range of intermediate flow rates, a transition flow regime takes place. The dominant feature is stagnation on the horizontal step face associated with significant splashing and a chaotic appearance. New criteria for the changes in flow regimes are presented. Transition flows are characterised by significant air entrainment and flow instabilities.

Keywords: stepped spillway, flow regimes, air entrainment, transition flow, air-water flows

1 INTRODUCTION

Stepped-channel spillways, staircase waste waterways, stepped spillways, and stepped chutes have been used for more than 3,000 years (CHANSON 2000,2001). A significant number of dams were built with overflow stepped spillways during the 19th century and early 20th century, before such spillways became outdated by progresses in hydraulic jump stilling basins. Recent advances in technology (e.g. RCC, polymer-coated gabion wire) have however triggered a regain of interest for stepped spillways. Unfortunately, though, much expertise had been lost in the past 60 years.

For a given stepped chute geometry, low discharges flow as a succession of free-falling jets (nappe flow) while a skimming flow regime is observed at large flow rates. Some researchers reported a range of transitory conditions between nappe and skimming flows: e.g., ELVIRO and MATEOS (1995), CHANSON (1996). OHTSU and YASUDA (1997) were probably the first to introduce the concept of "*transition flow*" regime although they did not elaborate on its flow properties. It was suggested that the transition flow is characterised by strong hydrodynamic fluctuations (CHANSON 1995).

It is the purpose of this paper to demonstrate the existence of the transition flow regime and to highlight the differences and specific features of this regime. The study is based upon new experiments performed in large-size facilities.

Basic flow regimes

The type of flow regime (i.e. nappe, transition or skimming flow) is a function of the discharge and step geometry. The writer re-analysed a large number of experimental observations of change in flow regimes (Fig. 1). (The re-analysis was based upon detailed descriptions and photographs, and new results.) All data points but one were obtained with flat horizontal steps. The legend (Fig. 1) indicates the type of transition: from nappe to transition flow (NA-TRA), from transition to skimming flow (TRA-SK). The indication (NA-SK) suggests that researchers ignored the transition flow regime.

The upper limit of nappe flow regime may be approximated as

$$\frac{d_c}{h} = 0.89 - 0.4 * \frac{h}{l}$$ Transition NA-TRA (1)

where dc is the critical depth, h is the step height and l is the step length, while the lower limit of skimming flow regime may be estimated as :

$$\frac{d_c}{h} = 1.2 - 0.325 * \frac{h}{l}$$ Transition TRA-SK (2)

Two issues must be clearly understood: {1} Equations (1) &(2) were deduced for flat horizontal steps with $0.05 \leq h/l \leq 1.7$; there is no information on their validity outside of that range; {2} Equations (1) & (2) characterise a change in flow regime for uniform or quasi-uniform flows ONLY; for rapidly varied flows, the results are inaccurate.

Experimental Investigations

New experiments were conducted at University of Queensland in a 24-m long 3.4º slope cascade (h = 0.07 m) and in a 2.7-m long 21.8º slope chute (h = 0.10 m) (Table 1). In each flume, waters are supplied by a pump controlled with adjustable frequency AC motor drive, enabling an accurate discharge adjustment in a closed-circuit system. The flow rates are measured with a Dall™ tube flowmeter and from the upstream head above crest with an accuracy of about 2%. Clear-water flow depths and velocities

were measured with a point gauge and a Prandtl-Pitot tube (∅ = 3.3 mm) respectively. Air-water flow properties were measured using a single-tip conductivity probe (∅ = 0.35 mm) aligned in the flow direction and excited by an air bubble detector (AS25240). The probe signal was scanned at 5-kHz for 180-s. The translation of the probes in the direction normal to the channel invert was controlled by a fine adjustment travelling mechanism connected to a MitutoyoTM digimatic scale unit (Ref. No. 572-503). The error on the vertical position of the probe was less than 0.025 mm. The accuracy on the longitudinal position of the probe was estimated as $\Delta x < \pm 0.5$ cm. The accuracy on the transverse position of the probe was less than 1 mm. Flow visualisations were conducted with a digital video-camera Sony™ DV-CCD DCR-TRV900 (speed: 25 fra/s, shutter: 1/4 to 1/10,000 s) and high-speed still photographs.

Both chutes are designed to operate either with nappe flows, transition flows or skimming flows. The present series of investigations were conducted specifically with transition flow conditions (Table 1).

2 EXPERIMENTAL RESULTS (1) FLOW PATTERNS

Experimental observations indicate that the appearance of the transition flow is neither that of nappe flow nor skimming flow. The flow does not exhibit the quasi-homogeneous appearance observed in skimming flow nor the succession of free-jets as in nappe flow. The dominant feature is the nappe stagnation onto each horizontal step face associated with strong splashing and spray (Fig. 2).

On the flat chute ($\alpha = 3.4^o$), the flow at the first drop was a deflected nappe associated with downstream shock wave propagation. On the following three steps, the flow was very chaotic and this flow establishment region was characterised by significant changes in flow properties from one step to the next one. For example, shock waves observed on Steps 2 were unseen on Step 3 and occurred sometimes on Step 4. The rate of energy dissipation was significant : i.e., $\Delta H/H_{max} \approx 30$ to 40% at the first three drops. Downstream, the flow becomes gradually-varied with slow variations of the flow properties from step to step, but significant longitudinal variations are observed on each step. At the step upstream end, the flow is characterised by a pool of recirculating waters, stagnation and significant spray and water deflection immediately downstream (Fig. 2). In the spray region, the depth-averaged mean air content Cmean may reach up to 40 %. Downstream the supercritical flow is decelerated up to the downstream step edge. Shock waves are observed in the supercritical flow region that are somehow similar to those observed in supercritical flows downstream of a single drop (e.g. CHANSON and TOOMBES 1998).

On a steep slope ($\alpha = 22^o$), the upstream flow is smooth and transparent. In the first few steps, the free-surface is undular in phase with the stepped geometry. Some aeration in the step corners is observed immediately upstream of the inception point of air entrainment. Downstream of the inception point, significant splashing is observed. At the lowest flow rates (e.g. dc/h = 0.77), some air cavities may exist and the air cavity shapes alternate from step to step. For example, a small air cavity may be observed followed by a larger nappe cavity at the downstream step, then a smaller one and so on. In the aerated flow region, the notable flow features are the nappe impact and stagnation point, and the spray and water droplets ejection downstream. There is no decelerated supercritical flow zone because the step length is too short (Fig. 2).

3 EXPERIMENTAL RESULTS (2) AIR-WATER FLOW PROPERTIES

Experimental observations suggest different flow behaviours for steep and flat chutes. Figures 3 and 4 present dimensionless distributions of void fractions and bubble count rates (i.e. number of bubbles detected per second) for $\alpha = 3.4^o$ and 22^o respectively.

On a flat chute ($\alpha = 3.4^o$), air concentration measurements show that the recirculation region is non-aerated. Downstream of the stagnation point, a substantial flow aeration is observed. Further downstream the supercritical flow is decelerated. In parts of the spray region and in the supercritical flow region, the air concentration distributions may be estimated as :

$$C = 1 - \tanh^2\left(K' - \frac{y}{2 * D' * Y_{90}}\right) \quad (3)$$

where tanh is the hyperbolic tangent function and y is the distance normal to the invert, Y90 is the distance where C = 90%. The dimensionless turbulent diffusivity D' and the integration constant K' are functions of the mean air content C_{mean} only (CHANSON 1997a). Figure 3 includes dimensionless distributions of bubble count rates $F_{ab}*d_c/V_c$, where F_{ab} is the bubble frequency, d_c is the critical depth and V_c is the critical flow velocity. For a given flow velocity and void fraction, the bubble count rate F_{ab} is inversely proportional to the mean bubble size, and directly proportional to the air-water specific interface area.

On a steep chute ($\alpha = 22^o$), the inception point of free-surface aeration is clearly defined. Downstream typical air-water flow properties are shown in Figure 4 where the dimensionless bubble count rate and void fraction are plotted as functions of the dimensionless distance y/dc, y being measured normal to the pseudo-bottom formed by the step edges. (All the data were

recorded at the step edges.) The dimensionless relationship between the void fraction C and the bubble frequency is also presented. It exhibits a quasi-parabolic shape which may be fitted by :

$$\frac{F_{ab}}{(F_{ab})_{max}} = 4 * C * (1 - C) \quad (4)$$

where the maximum bubble frequency (Fab)max is observed for C ≈ 50% (e.g. Fig. 5). For one particular flow condition (α = 22º, d_c/h = 0.77), a deflecting flow was observed 4 steps downstream of the inception point of air entrainment. Liquid fractions (i.e. (1-C)) greater than 10% were measured at distances up to 1.5*d_c. Some spray overtopped the 1.25-m high sidewalls. The nappe re-attached the main flow at the next downstream step edge.

4 DISCUSSION

Very rapid free-surface aeration was observed in the transition flow. Measured values of mean air concentration C_{mean} were in excess of 35% and 50% on the 3.4º and 22º chutes respectively. Such values are larger than equilibrium values acknowledged in skimming flows. The experimental results imply that chute sidewalls must be designed higher than in nappe flows or skimming flow for identical flow rates. Observed maximum bubble frequencies $(F_{ab})_{max}$ ranged from 60 to 180 Hz, values that are similar to those observed in smooth-invert chutes (CHANSON 1997b). This suggests that mean air bubble sizes are of the same of order of magnitude in smooth- and stepped-invert spillways.

Figure 6 presents longitudinal variations of clear-water velocity for both chutes. In each case a gradual decay in velocity is observed, although longitudinal velocity fluctuations occur along each step on the flat chute. On the steep chute (α = 22º), the experimental observations suggest an asymptotical value of U_w/V_c ~ 2.5 while the pseudo-asymptotic value is about U_w/V_c ~ 2.2 to 2.5 on the flat cascade (α = 3.4º). Overall the results provide practical information for the design of the downstream energy dissipator.

Although two prototype accidents and one failure were experienced with transition flow conditions (CHANSON 1995,2001), some engineers refuse to consider the risks of failures associated with hydrodynamic instabilities at transition between nappe and skimming flow even after large cracks were observed underneath two prototype spillway chutes. The above results demonstrate that the transition flow is characterised by a chaotic flow behaviour associated with rapid variations of the flow properties on each step. Such unsteady fluctuations are associated with pressure fluctuations on the step faces and fluid-structure interactions. Practically, a stepped spillway must be designed to avoid the transition flow regime, unless a rigorous hydraulic and structural modelling of the flow instabilities is conducted.

5 SUMMARY AND CONCLUSION

For intermediate flow rates, a transition flow regime may occur on a stepped spillway. The transition flow is characterised by strong stagnation on the horizontal step faces associated with downstream splashing. New experiments were conducted with two large size facilities (α = 3.4º and 22º) and the results provide information on the air-water flow properties of transition flows. Significant air entrainment takes place, in excess of observed levels in skimming flows. At the downstream end of the chutes, observed mean flow velocities were about U_w/V_c ~ 2.2 to 2.5 (Fig. 6).

Further the experimental study highlighted significant flow variations on each step, and some instabilities for one discharge. It is strongly recommended to avoid the design of stepped spillways with transition flow regime. Nonetheless the transition flow might be a suitable flow regime for aesthetical purposes (e.g. fountains) and for water treatment (e.g. aeration cascades) because of the strong splashing and free-surface aeration.

Acknowledgements

The writer acknowledges the assistance of M. EASTMAN and N. VAN SCHAGEN, and of Dr L. TOOMBES (Brisbane, Australia).

References

Chanson, H. (2001). “The Hydraulics of Stepped Chutes and Spillways.” Balkema Publ., The Netherlands.

Chanson, H. (2000). Jl of Hyd. Engrg., ASCE, Vol. 126, No. 9, pp. 636-637.

Chanson, H. (1997a). "Air Bubble Entrainment in Free-Surface Turbulent Shear Flows." Academic Press, London, UK.

Chanson, H. (1997b). Intl Jl of Multiphase Flow, Vol. 23, No. 1, pp. 193-203.

Chanson, H. (1996). Jl of Hyd. Res., IAHR, Vol. 34, No. 3, pp. 421-429.

Chanson, H. (1995). "Hydraulic Design of Stepped Cascades, Channels, Weirs and Spillways." Pergamon, Oxford, UK.

Chanson, H., and Toombes, L. (1998). Can. Jl of Civil Eng., Vol. 25, No. 5, pp. 956-966.

Elviro, V., and MATEOS, C. (1995). Intl Jl Hydropower & Dams, Vol. 2, No. 5, pp. 61-65.

Ohtsu, I.O., and Yasuda, Y. (1997). Proc. 27th IAHR Biennal Congress, San Francisco, USA, Theme D, pp. 583-588.

Table 1 Detailed experimental investigations of transition flows

Ref.	α	h	q_w	dc/h	Remarks
	deg.	m	m^2/s		
(1)	(2)	(3)	(4)	(5)	(6)
UQ	3.4	0.071	0.08	1.22	L = 24 m. W = 0.5 m. Supercritical inflow : do = 0.03 m. 19 flat horizontal steps (h=0.071, l = 1.2 m).
UQ	21.8	0.10			L = 2.7. W = 1 m. Smooth sidewall convergent (4.8:1) followed by broad-crest. Low upstream turbulence. 9 flat horizontal steps.
			0.102	1.0	Run Q2.
			0.080	0.87	Run Q3.
			0.066	0.77	Run Q4.

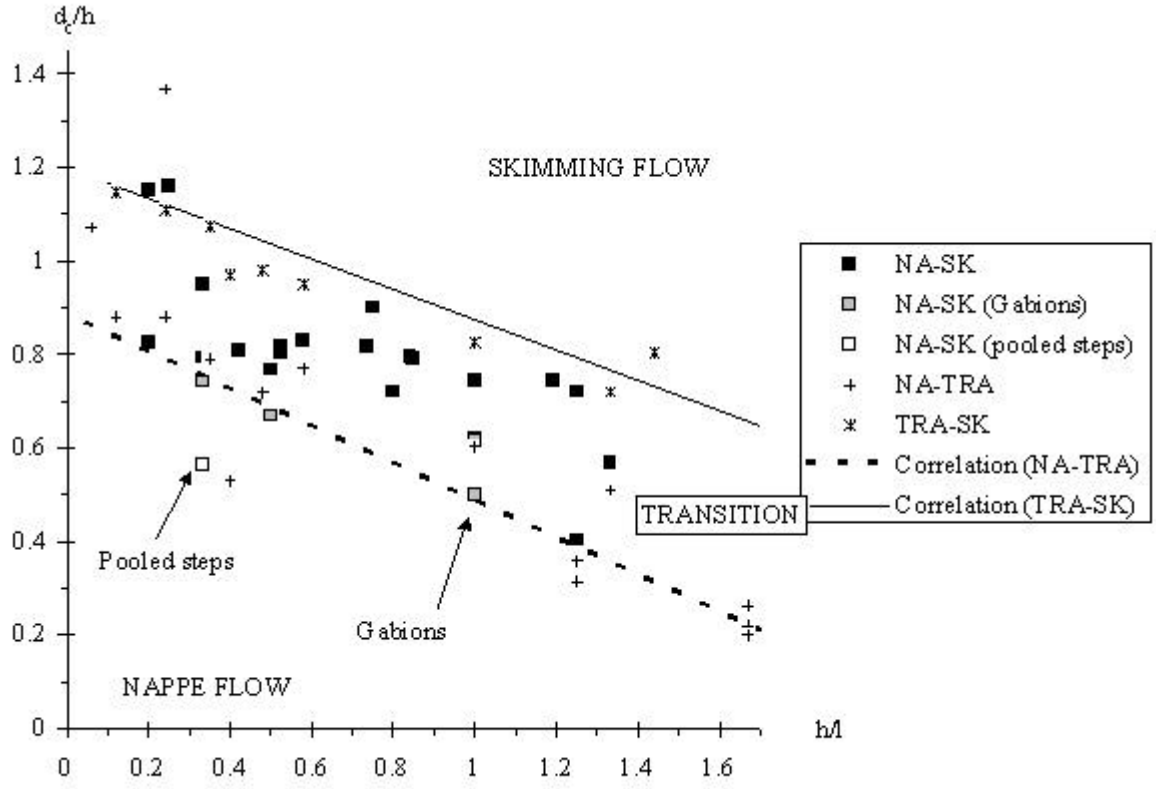

Fig. 1 Flow conditions for the transition from nappe to skimming flow - Summary of experimental data (after CHANSON 2001)

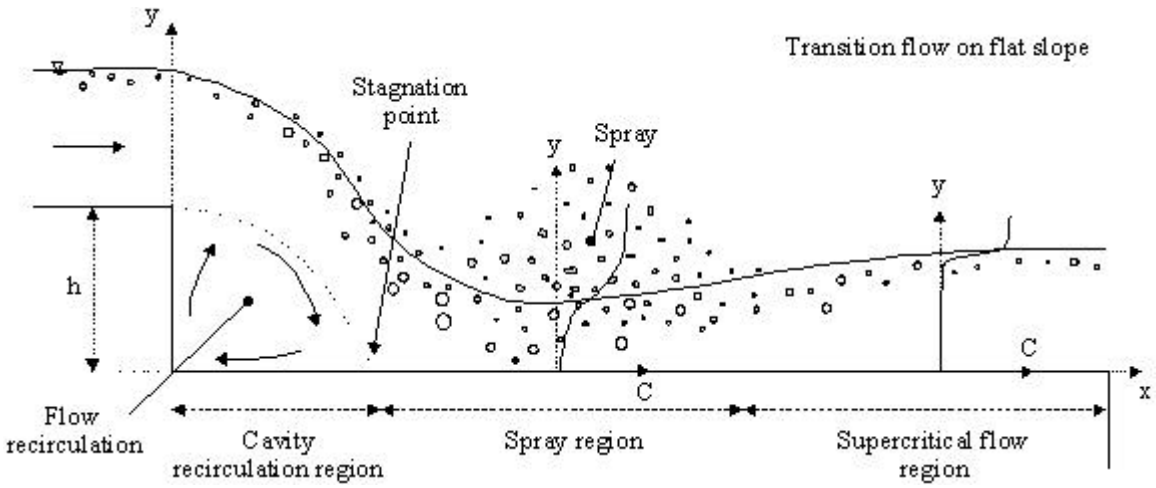

Fig. 2 Basic flow patterns in transition flows down a stepped chute

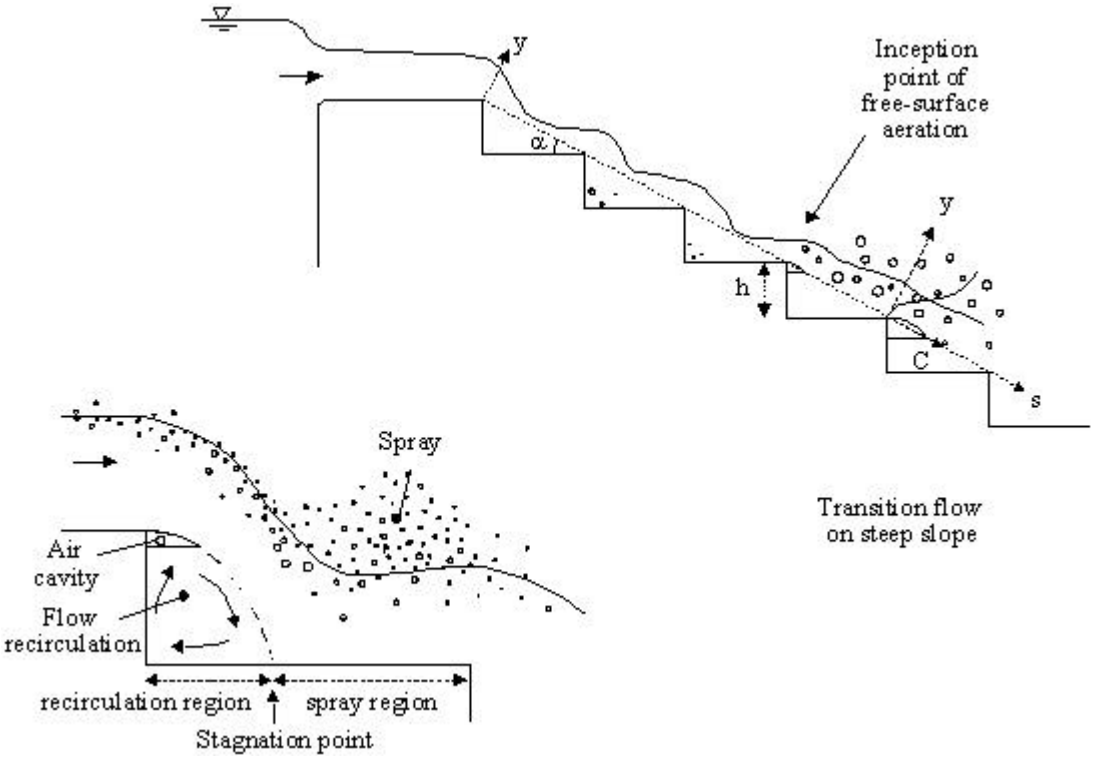

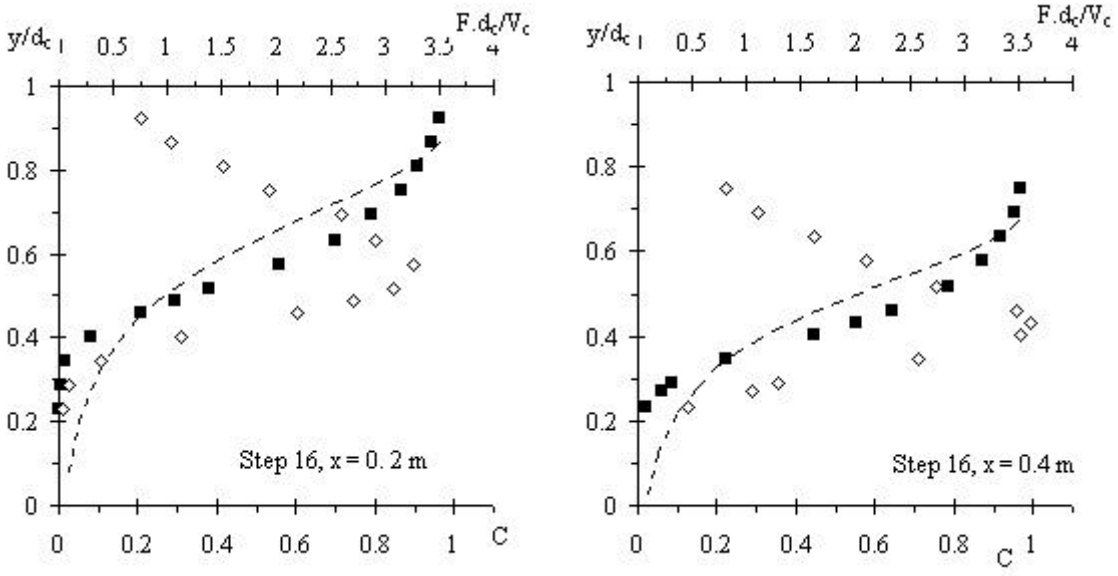

Fig. 3 Dimensionless air concentration and bubble frequency distributions (α = 3.4º, qw = 0.08 m2/s, Step No. 16) in impact zone (x = 0.2 and 0.4 m) and supercritical flow zone (x = 0.6 and 1 m) - Legend : black square = air concentration; white diamond = bubble frequency

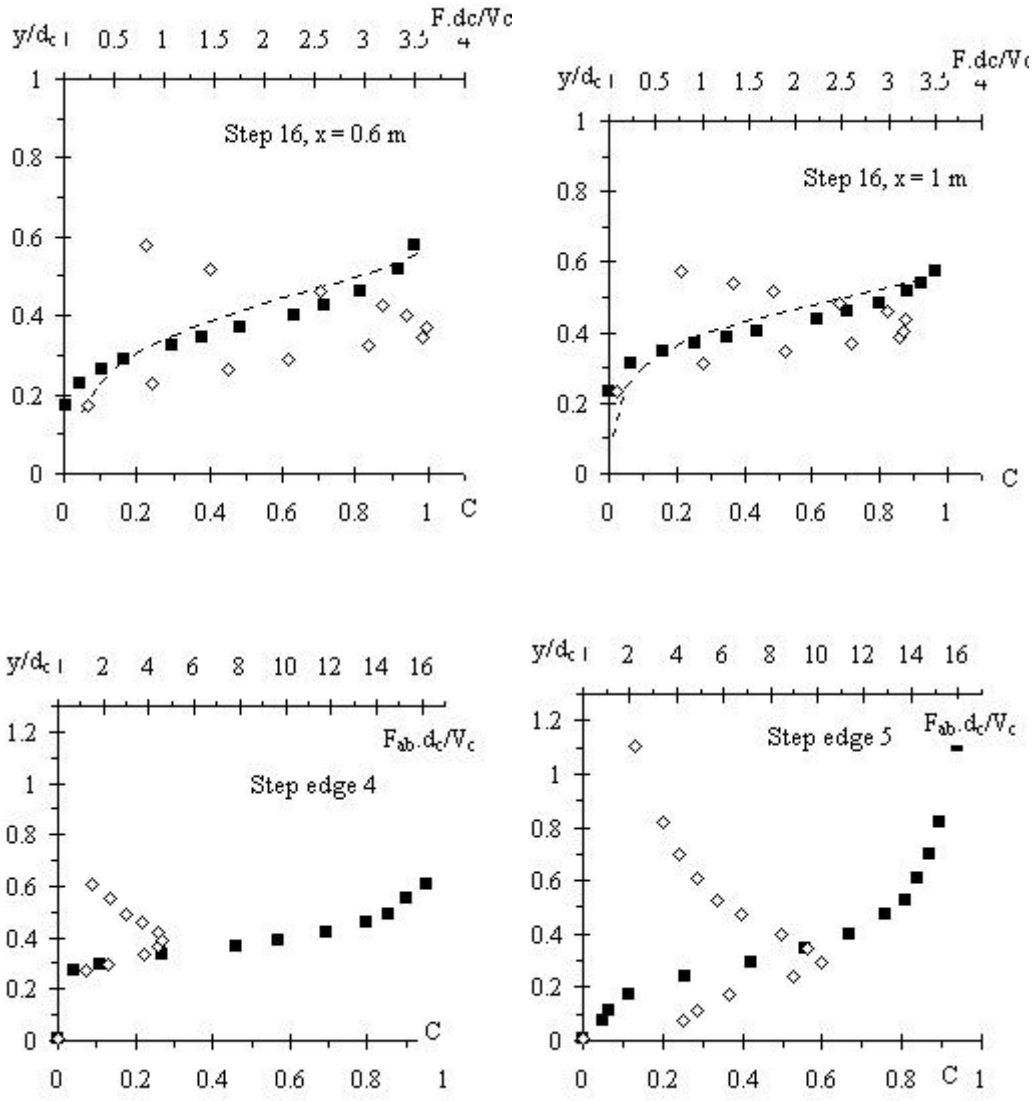

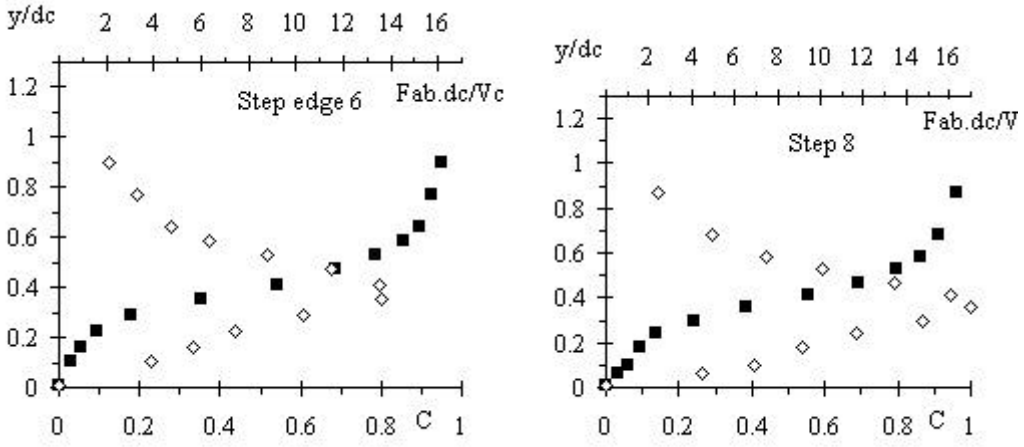

Fig. 4 Dimensionless air concentration and bubble frequency distributions (α = 22°, d_c/h = 0.87, data measured at step edge) - Legend: black square = air concentration; white diamond = bubble frequency

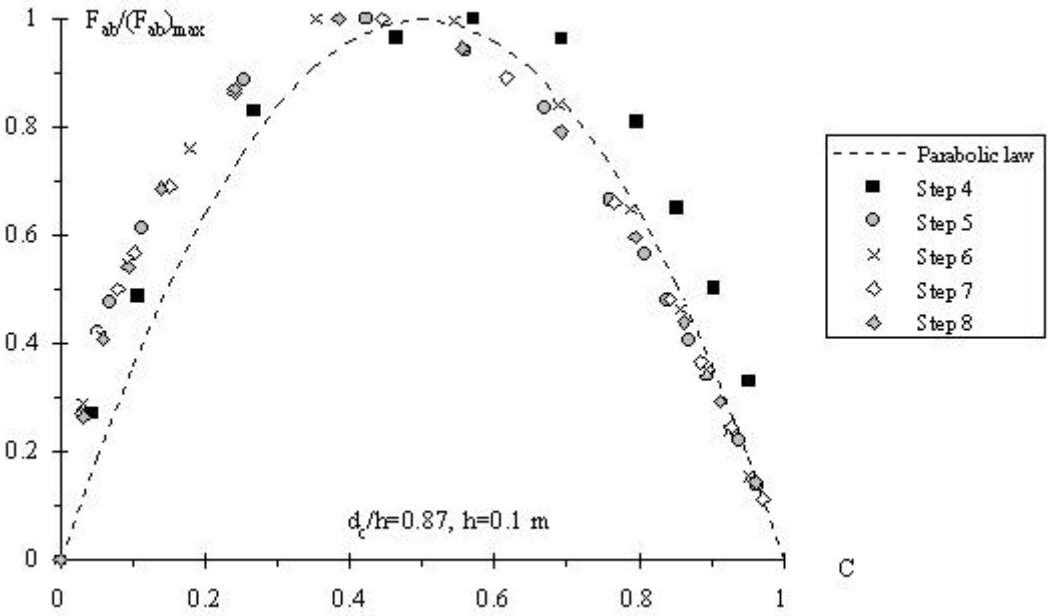

Fig. 5 Dimensionless relationship between air concentration and air bubble frequency

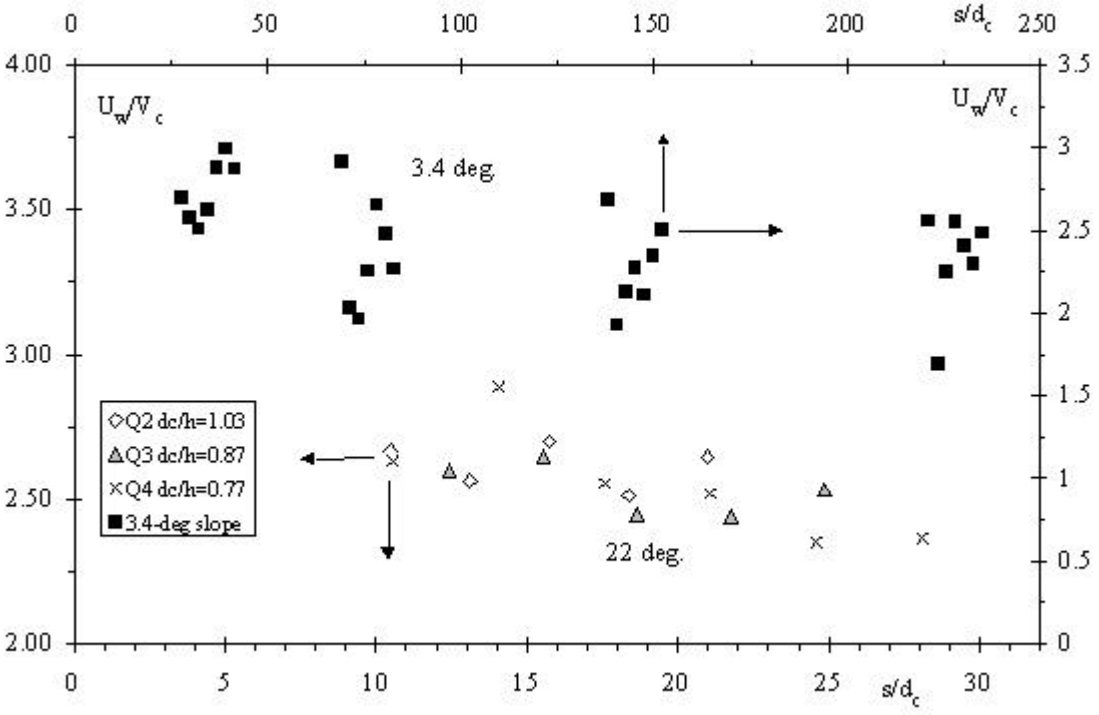

Fig. 6 Dimensionless clear-water flow velocity data